

Low Drive Voltage, Negative Chirp 40 Gb/s EA-Modulator/Widely-Tunable Laser Transmitter, Using Quantum-Well-Intermixing

J.W. Raring^{*}, L.A. Johansson[†], E.J. Skogen[†], M.N. Sysak[†], H.N. Poulsen[†], S.P. DenBaars^{*}, and L.A. Coldren^{*†}

^{*}Materials Dept. University of California, Santa Barbara, CA 93106

[†]ECE Dept. University of California, Santa Barbara, CA 93106

Phone: 805.893.7163, Fax: 805.893.4500, Email: jraring@engineering.ucsb.edu

Abstract: We present the first 40Gb/s widely-tunable EAM/laser transmitters demonstrating 1.0-1.5V_{Pt0P} drive, low-chirp, and under 0.5dB of power penalty for transmission through 2.3km of fiber. A robust quantum-well-intermixing technique was employed for the realization of these devices.

©2006 Optical Society of America

OCIS codes: (140.5960) Semiconductor lasers; (140.3600) Lasers, tunable; (250.5300) Photonic Integrated Circuits

1. INTRODUCTION

For the first time, an electroabsorption modulator (EAM) based widely-tunable transmitter demonstrating negative chirp performance at 40 Gb/s has been fabricated using a simple, robust quantum-well-intermixing (QWI) processing platform. The transmitter consists of a quantum-well (QW) EAM monolithically integrated with a widely-tunable sampled grating (SG) DBR laser. The EAMs demonstrated 3dB optical bandwidths of up to 39 GHz, low drive voltages (1.0-1.5 V_{Pt0P}), and 0.2- 0.5 dB of power penalty for 40 Gb/s transmission through 2.3km of fiber across the wide tuning range of the SG-DBR laser. The QWI method facilitates a simple fabrication sequence avoiding the traditional processing complexity necessary for the integration of negative chirp EAMs with diode lasers.

Electroabsorption-modulated lasers are candidate sources for 40 Gb/s very-short-reach (VSR) router to router interconnect applications, as they are compact, potentially low-cost, and can facilitate low drive voltages with high bandwidth [1]. The monolithic integration of EAMs with widely-tunable lasers allows for inventory reduction and wavelength agile functionality. A QW-based EAM exploits the quantum confined stark effect resulting in increased efficiency over bulk Franz-Keldysh type EAMs, and allows for the possibility of achieving negative chirp. Previous reports of 40 Gb/s QW-EAMs either did not include an integrated laser or included a single frequency distributed feedback (DFB) laser [1, 2, 3].

Butt-joint regrowth is the traditional method implemented to monolithically integrate QW-EAMs with lasers. This method involves the selective removal of the as-grown waveguide/multiple QW (MQW) region followed by the regrowth of waveguide/MQW material with the desired band edge. Although the butt-joint regrowth process does allow each integrated component to possess a unique band edge, the difficulty associated with matching thickness and achieving the desired composition to avoid reflection and loss at the interface is great [4]. Selective area growth is another technique used to realize multiple band edges across a wafer. However, in addition to the lack of abruptness of the transition region, the thickness of the waveguide changes from one region to the next therefore modulating the optical confinement factor of the device in the axial direction. Another method uses the detuning of the DFB laser Bragg wavelength from the absorption edge of the MQW, allowing the same active layer to be used in the laser and EAM. However, this method imposes a performance trade-off between the laser and EAM [3]. The relatively simple QWI process employed in this work enables optimal placement of the QW band-edge in the laser, EAM, and passive sections without disturbing the waveguide in the axial direction [5].

2. EXPERIMENT

The transmitter used in this work was the output stage of an integrated transceiver, which also contained an SOA/photodetector receiver [6]. The receiver consists of a low-confinement semiconductor optical amplifier (SOA) for high saturation power and a uni-traveling carrier (UTC) photodiode capable of 40 Gb/s operation. Details of the receiver structures are given in [7, 8]. Here we focus on the transmitter, which contains a five section widely tunable sampled-grating (SG) distributed Bragg reflector (DBR) laser followed by an EAM. The 5 sections of the SG-DBR laser are, from back to front in Fig. 1a, backside absorber, rear mirror, phase, gain, and front mirror. The phase and mirror sections function to tune the wavelength of the laser [5]. The lithographically defined mirrors make the SG-DBR laser ideal for monolithic integration.

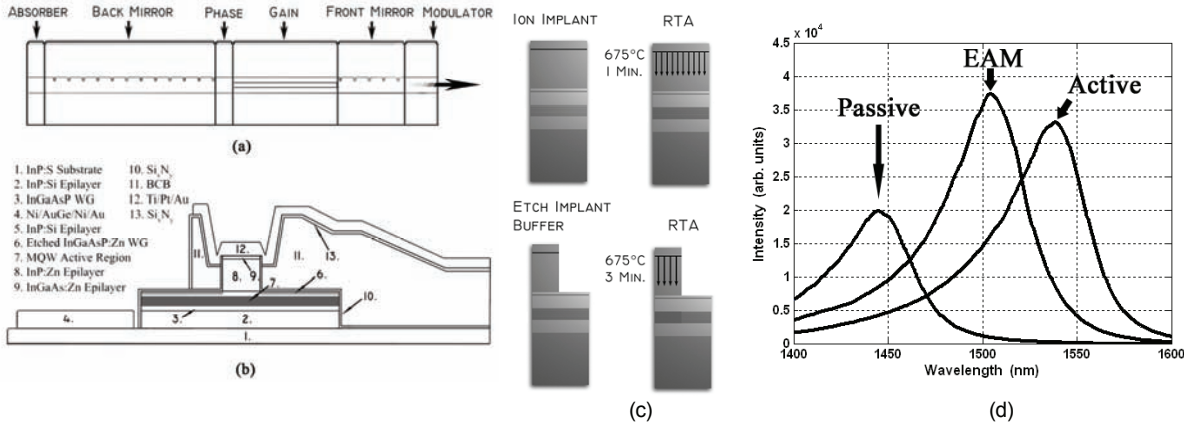


FIGURE 1. (a) Side view schematic of the SG-DBR/EAM device architecture. (b) Cross-sectional schematic of the 3 μm wide modulator sections. (c) Quantum well intermixing scheme used for device fabrication. (d) Photoluminescence of the as-grown active regions, partially intermixed EAM regions, and severely intermixed passive sections.

This work employs a modified ion-implantation enhanced QWI process described in [5]. In this process, point defects are created by ion implantation into an InP buffer layer over the MQW active region. During a high temperature anneal, the defects are diffused through the MQW region, promoting the interdiffusion of group V-atoms between the wells and barriers. The interdiffusion reshapes the QW profile resulting in a shift in the quantized energy levels in the well, and hence a shift in the band edge energy.

3. PROCESS

Two different epitaxial base structure MQW designs were explored in this work. The first consisted of 10 InGaAsP 6.5 nm compressively strained (0.9%) QWs and 8.0 nm tensile strained (0.3%) InGaAsP barriers. The second consisted of 15 InGaAsP 8.0 nm compressively strained (0.6%) QWs and 8.0 nm tensile strained (0.3%) InGaAsP barriers. Both MQW designs were centered within a 1.3Q waveguide. A standard surface ridge waveguide architecture was employed in the laser and EAM. A cross-section of the 3 μm wide EAM region is shown in Fig. 1b. Using the intermixing process detailed in [5] and illustrated in Fig. 1c, the as-grown MQW band-edge ($\lambda_{\text{PL}} = 1540\text{nm}$) was blue-shifted in the EAM ($\lambda_{\text{PL}} = 1505\text{nm}$) and passive regions ($\lambda_{\text{PL}} = 1440\text{nm}$) as shown in Fig. 1d.

4. RESULTS

The surface ridge SG-DBR lasers using the 10 MQW design demonstrated over 30 nm of tuning, threshold currents of 35 mA, and output powers of 15–30 mW at a gain section current of 150 mA. At this operating point, a side mode suppression ratio (SMSR) greater than 35 dB was achieved. The EAMs with a length of 125 μm demonstrated over 20 dB of DC extinction for wavelengths from 1535 nm to 1560 nm, with peak efficiencies of over 15 dB/V as shown in Fig. 2a for the 10 MQW device. The small signal response, shown in Fig. 2b, of the 10 and 15 MQW modulators terminated with 50 Ω demonstrated 3dB optical bandwidths of 39 GHz and 35 GHz, respectively. The broadband large-signal chirp parameter was characterized using Time Resolved Chirp (TRC) software for both MQW designs with 1.5 V_{PtoP} applied to the 10 MQW and 1.0 V_{PtoP} applied to the 15 MQW EAM. As shown in Fig.

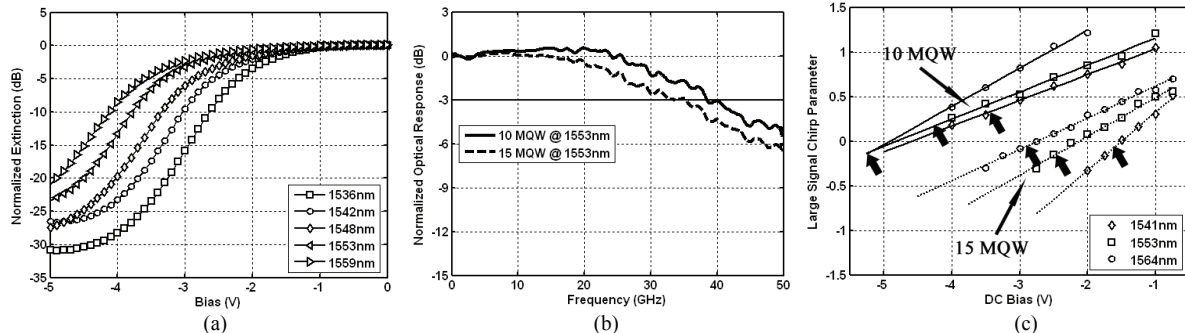


FIGURE 2. (a) Broadband DC extinction of 125 μm EAM with 10 MQW design. (b) Small signal response of 125 μm EAMs using 10 MQW and 15 MQW designs. (c) Broadband large signal chirp parameter of EAMs using the 10 MQW (1.5 V_{PtoP}) and 15 MQW (1.0 V_{PtoP}) designs with arrows indicating DC bias used for optimized 40 Gb/s eye diagrams shown in Fig. 3a for the 10 MQW EAM.

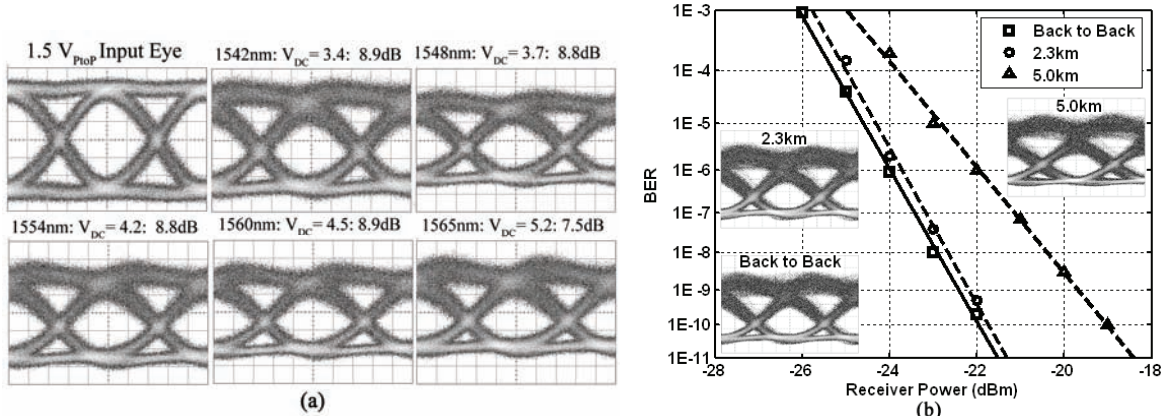


FIGURE. 3 (a) 40 Gb/s eye diagrams from 10 MQW device with a $1.5 \text{ V}_{\text{PtoP}}$ drive and average fiber-coupled output powers of -5dBm to 0dBm. The wavelength, DC bias, and extinction ratio are depicted. (b) Bit error rate measurements from 10 MQW device at 40 Gb/s with a $1.5 \text{ V}_{\text{PtoP}}$ drive and a wavelength of 1553nm. The back to back eye diagram along with the eye diagrams after transmission are shown as insets.

2c, the chirp parameter approaches zero and goes negative with increasing reverse bias for the QW-EAMs.

Non return to zero (NRZ) eye diagrams were taken at 40 Gb/s with a pseudo random bit sequence (PRBS) of $2^{31}-1$ over the tuning range of the SG-DBR lasers for both MQW designs. In Fig. 3a, the back to back input eye along with device output eyes are shown for the 10 MQW EAM with a $1.5 \text{ V}_{\text{PtoP}}$ drive and average fiber-coupled powers in the -5dBm to 0dBm range. Extinction ratios (ER) greater than 8.7dB are demonstrated for wavelengths up to 1560nm with DC bias levels ranging from 3.4V to 5.2V. The 15 MQW EAM required only a $1.0 \text{ V}_{\text{PtoP}}$ drive to achieve similar values of ER across the SG-DBR tuning range. The DC bias points for optimized eye diagrams are indicated on Fig. 2c to demonstrate the expected chirp at these operating points. As can be seen, the predicted chirp for the 10 MQW EAMs ranges from -0.1 to 0.3 and for the 15 MQW the chirp parameter is negative in all cases.

40 Gb/s bit error rate (BER) testing was performed on the 10 MQW transmitter for transmission through 2.3km and 5km of standard Corning SMF-28 fiber. A PRBS of 2^7-1 was used due to a noise floor in the bit-error rate test set-up at longer word lengths. In Fig. 3, the BER results and the respective eye diagrams for transmission through fiber are shown for a wavelength of 1553nm using a $1.5 \text{ V}_{\text{PtoP}}$ drive and a DC bias of 4.9V. The transmitter demonstrated between 0.2dB and 0.5dB of power penalty for transmission through 2.3km of fiber at wavelengths spanning from 1543nm to 1565nm. According to Fig. 2c, the operating points in this experiment were expected to provide slightly negative chirp. Upon increasing the transmission length to 5km, the power penalty increased to 3dB due to fiber dispersion.

5. CONCLUSION

For the first time, we have demonstrated high performance 40 Gb/s widely-tunable EAM/laser transmitters. The 10 MQW transmitters exhibited 39GHz of 3dB bandwidth, a $1.5 \text{ V}_{\text{PtoP}}$ drive, negative chirp, and low power penalty transmission through 2.3km of fiber across the tuning range of the laser. The 15 MQW device required lower drive voltages ($1.0 \text{ V}_{\text{PtoP}}$) and provided negative chirp at lower DC bias levels. This work was facilitated by a simple, robust QWI processing platform for the monolithic integration of blue-shifted QW-EAMs with SG-DBR lasers.

6. REFERENCES

- [1] M. Okuyasu, et al., "A 1550-nm 40-Gbit/s Electro-Absorption DFB Laser Diode Module for Transponders with Very Short Reach (<2 km) Applications" *Lasers and Electro-Optics Society, LEOS Technical Digest paper WG2*, 2004
- [2] H. Fukano, et al., "Very Low Driving Voltage InGaAlAs/InAlAs Electroabsorption Modulators Operating at 40 Gbit/s," *IEE Electron. Lett.*, vol. 41, No. 4, 2005.
- [3] P. Gerlach, et al., "40-Gbit/s Operation of Laser-Integrated Electroabsorption Modulator Using Identical InGaAlAs Quantum" *International Conference on Indium Phosphide and Related Materials*. Technical Digest. 2005
- [4] J. Binsma, et al., "Characterization of Butt-Joint InGaAsP Waveguides and Their Application to 1310 nm DBR-Type MQW Gain-Clamped Semiconductor Optical Amplifiers," *IEICE Trans. Electron.*, vol. E80-C, pp. 675-681, 1997.
- [5] E. Skogen, et al., "Post-Growth Control of the Quantum-Well Band Edge for the Monolithic Integration of Widely-Tunable Lasers and Electroabsorption Modulators," *IEEE J. Sel. Topics Quantum Electron.* *IEEE J. Sel. Topics in Quantum Electron.*, vol. 9, pp. 1183-1190, 2003.
- [6] J. Raring, et al., "Quantum Well Intermixing for Monolithic Integration: A Demonstration of Novel Widely-Tunable 10Gb/s Transmitters and Wavelength Converters," *Integrated Photonics Research Conf.*, San Francisco 2004.
- [7] J.W. Raring, et al., "Demonstration of high saturation power/high gain SOAs using quantum well intermixing and MOCVD regrowth," *IEE Electronics Letts.* vol.41, issue 24 pp. 1345-1346 Nov. 2005.
- [8] J.W. Raring, et al., "Design and Demonstration of Novel Quantum Well Intermixing Scheme for the Integration of UTC-Type Photodiodes with QW-Based Components", *IEEE Journal of Quantum Electronics*, Vol. 42, No. 2, pp. 171-181, 2005.